Estimation and Error Analysis of Woody Canopy Leaf Area Density Profiles Using 3-D Airborne and Ground-Based Scanning Lidar Remote-Sensing Techniques

Fumiki Hosoi, Yohei Nakai, and Kenji Omasa

***Abstract*—Vertical profiles of the leaf area density (LAD) of a Japanese zelkova canopy were estimated by combining airborne and portable ground-based light detection and ranging (lidar) data and using a voxel-based canopy profiling method. The profiles obtained by the two types of lidars complemented each other, eliminating blind regions and yielding more accurate LAD profiles than could be obtained by using each type of lidar alone. In the combined results, the mean absolute errors (MAEs) of LAD ranged from 0.20 to 0.42 m^2 m^{-3}, and the mean absolute percentage errors (MAPEs) of the leaf area index (LAI) ranged from 22.3% to 27.2%, for ground areas from 4 to 32 m^2, respectively. A laser beam coverage index Ω incorporating the lidar's beam settings and a beam attenuation factor was proposed. This index showed general applicability to explain the LAD estimation error for LAD measurements using different types of lidars and with different beam settings. Parts of the LAD profiles that were underestimated even when data from both lidars were combined were interpolated by using a Gaussian function. The interpolation yielded improved results for ground areas of 16 and 32 m^2; the respective MAEs of LAD were 0.17 and 0.11 m^2 m^{-3}, and the respective MAPEs of LAI were 8.0% and 9.4%. The proposed method improves lidar-derived LAD estimation and is adapted to broadleaved canopies. The index Ω was tested against an actual canopy scenario and could be used to determine appropriate lidar measurement settings when data from different sources of lidar data are combined to estimate LAD profiles.**

***Index Terms*—Airborne scanning light detection and ranging (lidar), composite remote sensing, laser beam coverage index, leaf area density (LAD), leaf area index (LAI), portable ground-based scanning lidar, three-dimensional (3-D), voxel-based canopy profiling (VCP).**

I. Introduction

THE plant canopy plays important functional roles in the cycling of materials and energy through photosynthesis and transpiration, the maintenance of plant microclimates, and the provision of habitats for various species [1]–[3]. Determining the vertical structure of the canopy is very important, because the 3-D composition of the canopy helps to sustain those functional roles [4]–[7]. The vertical canopy structure is often represented by the vertical distribution of the leaf area density (LAD) in each horizontal layer, defined as the distribution of the one-sided leaf area per unit of the horizontal layer volume [8]. Vertical integration of the LAD profile data yields the leaf area index (LAI).

Although various ways of measuring LAD and LAI have been used in previous works, the measurement of these parameters is still difficult. A direct method is stratified clipping of biomass samples [9]. Although this straightforward method gives accurate results, it has limited applicability in the field because it is destructive and very laborious. Another direct method involves 3-D digitizing by ultrasonic or electromagnetic devices, whereby geometric information is recorded in a 3-D spatial coordinate system by a pointer to the position of each plant component [10]–[12]. This technique can nondestructively provide detailed information about the 3-D structure of plants, but it is also labor intensive because numerous components must manually be measured, point by point. An indirect method, the gap-fraction method, is widely applied in field surveys by using commercially available tools such as cameras with fish-eye lenses and optical sensors (e.g., the LI-COR LAI-2000 Plant Canopy Analyzer) [13], [14]. This method, which is based on light transmittance through the canopy, allows automatic nondestructive estimation of LAI and LAD. However, the method also has a weak point because the accuracy of the measurement is affected by the spatial distribution of leaves and by sunlight conditions [15], [16].

Light detection and ranging (lidar), which is an active remote-sensing technique that uses a laser scanner, has also been applied to canopy measurements. The vertical profile of the structure of a forest canopy can be estimated by an airborne large-footprint lidar from the waveforms of the returned pulses [5], [17]. However, the image resolution is not fine enough to describe the canopy structure at the individual tree scale. Canopy structure has been measured more accurately by using an airborne small-footprint lidar, which has fine spatial resolution [18]–[29]. This type of lidar has been used for estimating the LAI values of several species of coniferous trees [30], [31] and crops [32]. However, these studies focused on LAI estimation rather than on the estimation of the vertical LAD profile, because they captured insufficient information about the vertical canopy structure to estimate the latter. Attempts have been made to measure vertical canopy profiles in eucalyptus

Manuscript received December 14, 2008; revised July 25, 2009 and November 2, 2009. First published February 17, 2010; current version published April 21, 2010.

The authors are with the Graduate School of Agricultural and Life Sciences, University of Tokyo, Tokyo 113-8657, Japan (e-mail: aomasa@mail.ecc.u-tokyo.ac.jp).

Color versions of one or more of the figures in this paper are available online at http://ieeexplore.ieee.org.

Digital Object Identifier 10.1109/TGRS.2009.2038372

[33] and Douglas-fir [34] forests by using an airborne small-footprint lidar. However, the profiles showed little response from the lower canopy levels, known to be present in the actual foliage profile, apparently because the laser beams from the lidar could not reach the lower canopy due to obstruction by the upper canopy. As a result, the lower canopy level is regarded as a blind region to airborne lidar measurement. Thus, the measurement of the vertical LAD profile by airborne small-footprint lidar is still problematic.

Portable ground-based lidars have been used for accurate measurements of whole plants and vegetation canopies [7], [26], [35]–[42]. A ground-based lidar is expected to compensate for the weaknesses of an airborne lidar in LAD estimation, because its fine spatial and range resolutions and small beam size permit measurement of the inner canopies of trees, allowing an accurate estimation of LAD profiles. Portable ground-based scanning lidars have been applied to the measurement of both LAI [33], [43] and LAD profiles [44]–[47] by the gap-fraction method. However, the estimates obtained were insufficiently accurate because it was difficult to evenly illuminate the full canopy. The results were also affected by the nonuniformity of the actual foliage distribution and the presence of nonphotosynthetic tissue.

Three-dimensional imaging by portable ground-based scanning lidars has been demonstrated to provide accurate estimates of LAD based on the voxel-based canopy profiling (VCP) method [7], [37]–[39]. In this method, the canopy is fully and evenly scanned by using optimally inclined laser beams emitted from several points surrounding the canopy. Information about the laser traces is included in a 3-D array of voxels. A voxel can refer to 1) the presence of lidar data or 2) one or more laser beams passing without touching the canopy [37]. Based on the voxels, LAD profiles and the LAI of individual trees can accurately be estimated by counting the frequency of contact between the laser beams and foliage within the canopy in each horizontal layer. This method has been tested on a broadleaved woody canopy tree [38], in a study in which several lidar positions were established both on the ground and 10 m above the ground. The measurements on the ground yielded good estimates when a sufficient number of laser beams penetrated the full canopy, but the ground-level measurements showed an overall tendency to underestimate the upper canopy, because the laser beams were obstructed by the middle and lower parts of the target canopy itself and the other trees surrounding the target, keeping the beams from adequately reaching the upper canopy. Thus, the upper part of a woody canopy often becomes a blind region in ground-level lidar measurement, a situation opposite to that in airborne lidar measurement. Consequently, better LAD results were obtained in this study [38] by combining the measurements obtained at the ground level with those obtained at 10 m above the ground. The results suggested that above-ground measurement can complement ground-level measurement to eliminate blind regions. However, it is difficult in the field to set portable ground-based lidar systems at high above-ground positions. Meanwhile, another study [26] showed that ground-level lidar measurements could effectively be combined with above-ground lidar measurements obtained by an airborne scanning lidar. By combining the data from both types of lidar, a 3-D model of standing trees without any blind region could be produced, and some variables such as the canopy volume, the trunk volume, and the canopy cross-sectional area could be estimated. In this study [26], only an outer surface of the canopy was reproduced as a 3-D model. Such a model cannot be used for LAD estimation because information on the internal canopy is required for LAD estimation.

The results in [26] and [38] indicate that the combination of airborne and portable ground-based scanning lidars could potentially allow an accurate estimation of LAD by eliminating the blind regions of each lidar. Combining both lidar systems requires the appropriate determination of the measurement configuration (e.g., laser beam settings and lidar position) according to the canopy structure to obtain more accurate LAD estimates. A criterion is thus needed but should require being commonly applicable to both types of lidar system with different characteristics. However, such criterion has not yet been proposed.

In the present study, we estimated the LAD in a woody canopy by data from both airborne and portable ground-based lidars and using the VCP method. We then evaluated the accuracy of the LAD estimation by comparing the results of each separate lidar with those of the combined lidars. The results of the evaluation were used to establish a criterion for determining the appropriate lidar measurement settings applicable to different types of lidars, and an index that relates lidar setting values to the accuracy of LAD estimates was proposed. In addition, to further improve the accuracy of the composite results, we applied Gaussian fitting to the composite profiles.

II. Materials and Methods

A. Study Site and Direct Measurement of LAD

The study was carried out in a mixed plantation with nearly flat topography in Ibaraki Prefecture, 40 km northeast of central Metropolitan Tokyo, Japan $(35^\circ 59'\mathrm{N}, 140^\circ 02'\mathrm{E})$. The dominant tree species were Japanese cedar (*Cryptomeria japonica* [L.f.] D. Don), Japanese red pine (*Pinus densiflora* Siebold & Zuccarini), ginkgo (*Ginkgo biloba* Linnaeus), and Japanese zelkova (*Zelkova serrata* [Thunberg] Makino). The understory included grasses, forbs, and young evergreen trees such as *Camellia japonica* Linnaeus, *Ilex integra* Thunberg, and *Ternstroemia gymnanthera* Sprague. A Japanese zelkova canopy was chosen for measurement, and a 4 m $\times$ 8 m measurement plot was established beneath the canopy. The measurement plot was divided into eight 2 m $\times$ 2 m quadrats, and then, the region above the plot was divided into 128 cells (each 2 m $\times$ 2 m $\times$ 0.5 m high) between the heights of 5 and 13 m. The actual LAD in each cell was directly measured by stratified clipping in September 2005, the month following the lidar measurements of the leafy canopy. Details about the measurement plot and the direct measurement can be found in [38].

B. Measurements Using Portable Ground-Based and Airborne Scanning Lidars

Measurements using portable ground-based scanning lidars were conducted in August 2005 (leafy condition) and

February 2006 (leafless condition), as reported in [38]. The measurement plot and the area around the plot were also scanned in August 2005 from above by a lidar mounted on a helicopter (ALTM 3100 DC, Optech Company, and Aero Asahi Company, Japan). The airborne lidar calculated the distance to a target by the time-of-flight method and had four receiving modes—the first-, second-, third-, and last-pulse modes—in which the first, second, third, and last returned laser pulses, respectively, were detected. Laser pulses returned from the upper canopy were received as the first-pulse mode, so only the first-pulse-mode data were used in this study. The laser wavelength was 1064 nm, and its repetition frequency was 50 000 Hz. The scanning frequency and angle were set to 25 Hz and 20.0°, respectively. The flight speed and height were 50 km/h and 400 m, respectively. The range accuracy and horizontal accuracy were within 15 and 13 cm, respectively. The latter was calculated from the angular accuracy of the scanning system. The beam divergence was 1.0 mrad, and the footprint diameter on the ground was estimated to be about 0.40 m. The footprint interval, i.e., the distance between centers of adjacent laser beams on the ground, was 0.29 m in the direction of the scan and 0.26 m in the direction of flight. The 3-D geographic position was determined with helicopter-borne inertial measurement unit and high-resolution Global Positioning System receivers, both in the helicopter and on the ground.

C. Computation of LAD From Portable Ground-Based and Airborne Scanning Lidar Data

1) Data Registration and Removal of Nonphotosynthetic Tissues: The 3-D point cloud data obtained by airborne and portable ground-based lidars were registered into a common coordinate system using the iterative closest point algorithm [48]. The scans done with the portable ground-based lidar in August 2005 oriented at a central zenith angle of 57.8° permitted effective correction for leaf inclination without angle measurements [37], [38] and were used for the registration. Nonphotosynthetic tissues such as trunks and branches and understory were excluded with a method similar to the one found in [38]. Then, the voxel-based computation of LAD described below was conducted separately for the portable and airborne lidar data.

2) Voxel-Based Computation of LAD: LAD computation from portable ground-based lidars has been previously reported in [38], with a voxel size of $5 \times 5 \times 5$ mm. A similar computation process was applied to airborne lidar data with a voxel size of $100 \times 100 \times 100$ mm. The voxel size was chosen to be at least finer than the lidar spatial resolution to adequately convert the airborne lidar data to the voxel representation. In the computation for airborne lidar data, the influence of the leaf inclination angle and laser beam direction was corrected by using the correction factor of $\cos(\theta_{lmn})[G(\theta_{lmn})]^{-1}$, where θ_{lmn} is the mean zenith angle for all laser beam incidences within a cell, and $G(\theta_{lmn})$ is the mean projection of a unit leaf area on a plane perpendicular to the direction of the laser beam at θ_{lmn} [8], [13], [14], [16]. To determine the correction factor, θ_{lmn} was set to 180° (i.e., vertical), and the distribution of leaf inclination angles obtained in [38] was used.

3) Evaluation of the Accuracy of the Lidar-Derived LAD: From the LAD values of each lidar computed for each of the cells, vertical LAD profiles were estimated for each type of lidar for ground areas of 4, 8, 16, and 32 m^2, corresponding to one, two, four, and eight quadrats, respectively. For ground areas of 8 m^2 or more, the LAD profiles were obtained by horizontally averaging the LAD profiles of as many adjacent quadrats as corresponded to the ground area. For instance, an LAD profile for the ground area of 16 m^2 was obtained by averaging the LAD profiles of four horizontally adjacent quadrats. Thus, by combining adjacent quadrats, four different LAD profiles were estimated for a ground area of 8 m^2. Similarly, four different LAD profiles were also estimated for a ground area of 16 m^2. In the case of the ground area of 32 m^2—that is, the whole region of the measurement plot—just one LAD profile was estimated. The accuracy of the LAD profiles estimated for each ground area was evaluated by comparing the estimated and actual profiles and calculating the mean absolute error (MAE). Vertical integration of each LAD profile yielded the LAI, and the mean absolute percentage error (MAPE) of the LAI was also estimated by comparing the actual values with the estimated values for each ground area.

To obtain more accurate LAD profiles, the profiles derived from the two types of lidars were combined, with the LAD values from the portable ground-based lidar data being replaced with those from the airborne lidar data for heights over 10 m. The accuracy of the composite profiles of the two lidars was evaluated for ground areas of 4 to 32 m^2 by comparing the MAE values. The LAI values for all ground areas were derived by vertically integrating the composite profiles, and their MAPE values were compared.

D. Derivation of the Laser Beam Coverage Index

The evaluation of LAD estimation accuracy showed that a sufficient ground area for applying the composite method was 16 m^2 or more. Then, an index that was related to the LAD estimation error was derived for the ground areas of 16 and 32 m^2. On the assumption that the LAD estimation error is affected by the laser beam coverage within the canopy, three factors that relate to the coverage were selected: the horizontally projected area of the laser beam (A_{beam}), the number of incident laser beams from above (airborne lidar) or below (portable ground-based lidar) the canopy per unit area of a horizontal plane (N), and a laser beam attenuation factor $(K \cdot \mathrm{LAI}_{\mathrm{cum}})$. In the laser beam attenuation factor, K is a parameter for the influence of the leaf inclination angle and the laser beam direction on laser beam attenuation and is equivalent to the inverse of the correction factor $\cos(\theta_{lmn})\ [G(\theta_{lmn})]^{-1}$, described in Section II-C2. $\mathrm{LAI}_{\mathrm{cum}}$ is the lidar-derived cumulative LAI at a certain height. K and $\mathrm{LAI}_{\mathrm{cum}}$ reflect the structural attributes of the canopy, while A_{beam} and N relate to the laser beam settings. The laser beam coverage index Ω was made in relation to these three factors as follows:

$$\Omega = A_{\mathrm{beam}} \times N \exp(-K \cdot \mathrm{LAI}_{\mathrm{cum}}). \tag{1}$$

The index Ω is defined as the total horizontally projected area of the incident laser beams per unit area of a horizontal plane

within the canopy at a certain height. This is also translated as the proportion of the area of a horizontal plane within the canopy covered by laser beams at a certain height. A_{beam} and N were determined from the laser beam settings of each lidar. $K \cdot \mathrm{LAI}_{\mathrm{cum}}$ was calculated for each height by using the voxel attributes as follows (see [37]):

$$K \cdot \mathrm{LAI}_{\mathrm{cum}} = \sum_{k=m_h}^{m_{\mathrm{top}}} \frac{n_I(k)}{n_I(k) + n_p(k)}$$

for airborne lidar data (2)

$$K \cdot \mathrm{LAI}_{\mathrm{cum}} = \sum_{k=m_{\mathrm{bottom}}}^{m_h} \frac{n_I(k)}{n_I(k) + n_p(k)}$$

for portable ground-based lidar data (3)

where $n_I(k)$ is the numbers of voxels at which laser beams were intercepted, and $n_P(k)$ is the ones through which laser beams passed. m_h, m_{top}, and m_{bottom} are the voxel coordinates on the vertical axis equivalent to height h and the heights of the canopy top ($= 12.5$ m) and bottom ($= 5$ m). Ω was calculated for each height in regions corresponding to the LAD profiles estimated for ground areas of 16 and 32 m^2. Then, the relationships between Ω and the absolute errors of the corresponding LAD estimates were investigated for each type of lidar.

E. Interpolation

For ground areas of 16 and 32 m^2, the composite profiles of the two lidars underestimated the LAD at heights of around 10 m, a height corresponding to the peak of the actual LAD profile. The underestimated parts of the profiles were interpolated by using the following Gaussian function:

$$f(h) = a + b \exp \frac{(h - h_p)^2}{2c^2} \quad (4)$$

where h is the height, h_p is the height of the Gaussian function peak, and a to c are parameters that determine the form of the fitting function. The Gaussian function was chosen for the interpolation, since the Gaussian function has been used as a function that fits vertical LAD profiles of broadleaved canopies in a previous study [49]. To determine the function, several points had to be picked up from the composite profile. The LAD profiles derived from each lidar used to obtain the composite profile had a peak above (in the case of the airborne lidar) or below (in the case of the portable ground-based lidar) 10 m. By using these two peaks from the profiles of the two lidars, four to eight points were picked up from the composite profile and used in the interpolation as follows:

1) four points, i.e., the two peaks (one from the airborne lidar profile and one from the portable ground-based lidar LAD profile), a point 50 cm higher than the airborne lidar profile peak, and one 50 cm lower than the portable ground-based lidar profile peak (corresponding to points B′, C′, B, and C in Fig. 2);

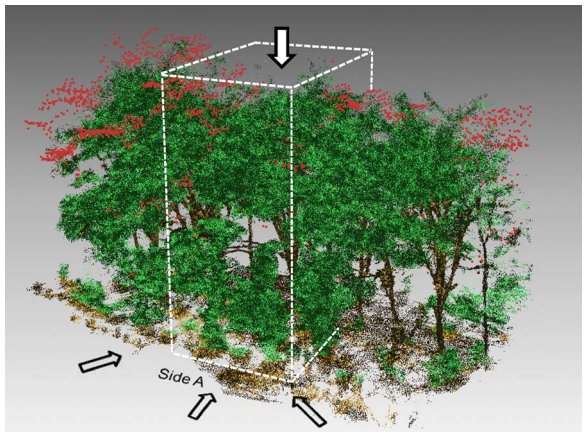

Fig. 1. Three-dimensional image of the Japanese zelkova canopy at the study site. This image was obtained by the registration of the images measured from above with the airborne lidar and from the six ground positions with the portable ground-based lidar. White dots represent the data obtained from the airborne lidar and gray and black dots represent the data from the ground-based lidar (in the online version of this paper, leaves are green, and other parts are brown for the ground-based lidar data, and the data obtained from the airborne lidar are colored red). Shading effect was added to this image by changing the brightness of each point. The number of data from the airborne lidar was quite less than the one from the portable ground-based lidar. The area enclosed by the broken white line corresponds to the measurement plot. Arrows show the directions of lidar scanning from side A on the ground and from above the canopy.

2) six points, i.e., the four points in (1), one 100 cm higher than the airborne lidar profile peak, and one 100 cm lower than the portable ground-based lidar profile peak (corresponding to points B′ to D′ and B to D in Fig. 2);
3) eight points, i.e., the six points in (2), one 150 cm higher than the airborne lidar profile peak, and one 150 cm lower than the portable ground-based lidar profile peak (corresponding to points B′ to E′ and B to E in Fig. 2).

In each point set (sets 1–3), parameters h_p and a to c were determined by the least-squares method to interpolate the underestimated parts of the composite profiles. The relative accuracy of the interpolation with each point set was evaluated by comparing the MAE values. The LAI values of the interpolated profiles were also estimated by vertical integration, and their MAPEs were evaluated.

III. Results

Fig. 1 shows the 3-D lidar image of the zelkova canopy after the registration of the images measured from the upper air by using the airborne lidar and from the six ground positions by using the portable ground-based lidar. For the ground-based lidar data, each tissue is clearly distinguishable because of the fine resolution of the image. The number of data obtained from the airborne lidar was quite less than the one of the portable ground-based lidar due to the difference in laser beam density between the two lidars.

Fig. 2 shows the LAD profiles for the entire measurement plot (32 m^2), obtained from actual measurements and from the two lidars. The portable ground-based lidar data and the actual ones were cited from [38]. LAD estimates from the airborne and portable ground-based lidar data agreed well with the actual values for the upper and lower canopies, respectively,

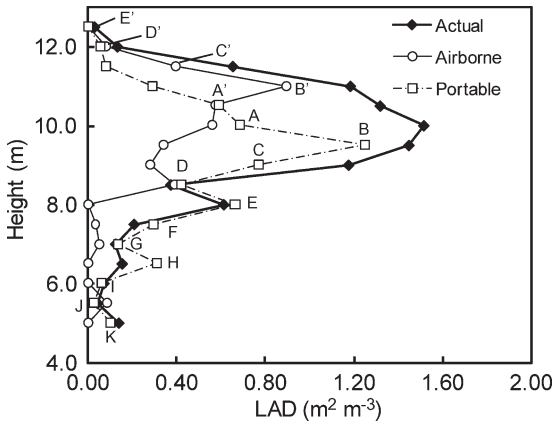

Fig. 2. Comparison of LAD profiles for the measurement plot estimated from airborne and portable ground-based lidar measurements and the actual LAD profile. The portable ground-based lidar data and the actual ones were cited from [38]. Points A to K and A′ to E′ indicate the points corresponding to the composite profile.

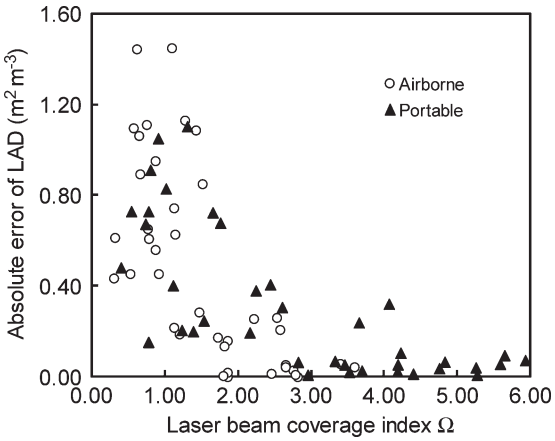

Fig. 4. Relationship between the laser beam coverage index Ω ($= A_{\mathrm{beam}} \times N \exp(-K\ \mathrm{LAI}_{\mathrm{cum}})$, given in (1), and the absolute errors of LAD in all airborne and portable ground-based lidar measurements for ground areas of 16 and 32 m^2.

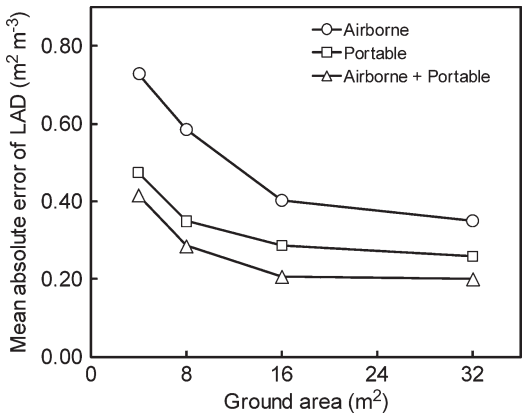

Fig. 3. Relationships between the ground area used for the LAD measurement and the MAEs of LAD for profiles obtained by the airborne lidar and the portable ground-based lidar and the composite profile.

but underestimated the values at around 10-m height. As a result, the peaks of the airborne and portable ground-based lidar profiles were above and below, respectively, the peak of the profile of actual measurements. The MAEs of the airborne lidar and portable ground-based lidar profiles were 0.35 and 0.26 $\mathrm{m}^2\ \mathrm{m}^{-3}$, respectively, and the MAE of the composite profile based on the data of both lidars was 0.20 $\mathrm{m}^2\ \mathrm{m}^{-3}$ (A to K and A′ to E′ in Fig. 2 indicate the points corresponding to the composite profile).

Fig. 3 shows the relationships between the measurement ground area and the MAEs of LAD obtained with different types of lidar and from the composite data without interpolation, as shown in Fig. 2. Comparison of data between the two lidars showed that the MAEs of the airborne lidar were larger than those of the portable ground-based lidar for all ground areas, and the LAD estimates in the composite profile had the lowest MAEs for all ground areas. The MAEs associated with the LAD profile of each lidar and with the composite profile were almost constant for ground areas of 16 m^2 or more but increased in relation to ground area for ground areas of less than 16 m^2. In addition, the rate of increase in the MAE for ground areas of less than 16 m^2 was higher with the airborne lidar than with the portable ground-based lidar. The MAPEs of LAI for ground areas of 4, 8, 16, and 32 m^2 were, respectively, 50.8%, 51.9%, 56.7%, and 59.8% for airborne lidar; 36.7%, 36.6%, 36.8%, and 37.2% for portable ground-based lidar; and 22.3%, 25.5%, 25.7%, and 27.2% for the composite profiles.

The relationships between the laser beam coverage index Ω [see (1)] and the absolute error of the LAD estimates of each lidar for ground areas of 16 and 32 m^2 are shown in Fig. 4. In spite of the different laser beam settings of the two lidars, the points from both lidars in the scatter plot were found in the same general region on the plot, indicating that the relationship between the index Ω and the LAD estimation error was similar between the two lidars. The absolute errors of both lidars began to drastically increase when Ω decreased to around 1.0. Large errors were associated with values of Ω less than or equal to approximately 1.0, whereas smaller errors were associated with values of Ω increased above 2.0.

Fig. 5(a) shows examples of the composite LAD profile for the ground area of 16 m^2 and the profile interpolated with a Gaussian function. For this interpolation, four points were picked up from the composite profile, with the result that the underestimated part of the composite LAD profile was improved by the interpolation, decreasing the MAE from 0.16 to 0.13 $\mathrm{m}^2\ \mathrm{m}^{-3}$. The MAE of all four profiles for the ground area of 16 m^2 decreased from 0.21 to 0.17 $\mathrm{m}^2\ \mathrm{m}^{-3}$, and the MAPE of LAI decreased from 25.7% to 8.0%. A similar improvement can also be observed in the profiles for the whole measurement plot (a ground area of 32 m^2 in Fig. 5(b); the actual LAD profile was cited from [38]). In this interpolation as well, four points were picked up from the composite profile. The MAE was decreased from 0.20 to 0.11 $\mathrm{m}^2\ \mathrm{m}^{-3}$, and the absolute error of LAI was also decreased, from 27.2% to 9.4%, by the interpolation.

The relationship between the number of points picked up for the Gaussian interpolation and the MAE of LAD after interpolation was evaluated for ground areas of 16 and 32 m^2. The MAEs in four, six, and eight picked-up points were, respectively, 0.16, 0.16, and 0.17 $\mathrm{m}^2\ \mathrm{m}^{-3}$ in a ground area of

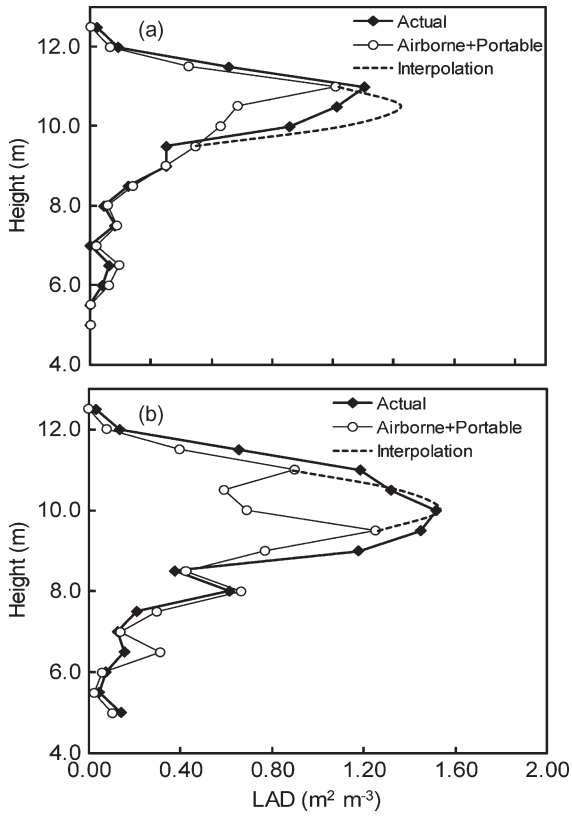

Fig. 5. Comparison of the composite LAD profile obtained by combining data measurement from the airborne and portable ground-based lidars, the profile obtained by interpolation of the composite profile by a Gaussian function, and the actual profile. (a) Examples for a ground area of 16 m^2 and (b) 32 m^2. The actual LAD profile at 32 m^2 was cited from [38].

16 m^2 and 0.11, 0.11, and 0.13 m^2 m^{-3} in a ground area of 32 m^2. For both ground areas, the MAEs were similar when either four or six points were picked up, and the MAE slightly increased when eight points were picked up.

Fig. 6 shows the MAEs of LAD estimates for ground areas of 16 and 32 m^2 for four different cases. The MAE decreased for both ground areas in the order airborne lidar $>$ portable ground-based lidar $>$ the composite of both lidars without interpolation $>$ the composite with interpolation using four picked-up points. This result clearly shows that the LAD estimation accuracy was improved by using the composite of the two lidars and then interpolating the composite profile by using a Gaussian function.

IV. Discussion

In the case of the studied canopy, the whole canopy could not be covered by either lidar by itself (Fig. 2), because the canopy at around 10-m height obstructed laser beams from the airborne lidar from reaching the lower canopy, and those from the portable ground-based lidar from reaching the upper canopy. The accuracy of the LAD profiles was improved (as shown in Fig. 3) by combining the profiles of the two lidars, so that they complemented each other, eliminating blind regions. However, ground areas of less than 16 m^2 were not suitable candidates for this technique (Fig. 3), because the error

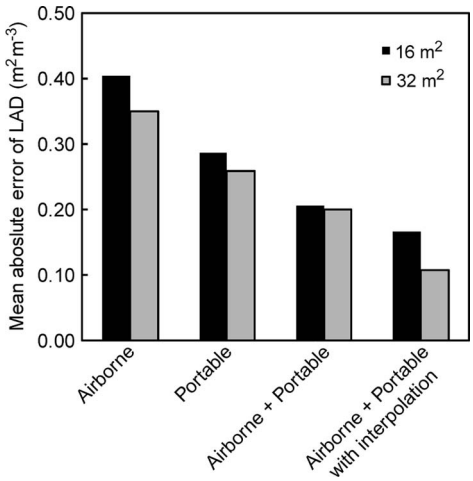

Fig. 6. Comparison of MAEs of LAD estimates for ground areas of 16 and 32 m^2 among airborne lidar measurements, portable ground-based lidar measurements, and the composite of the lidar measurements and after interpolation of the composite by a Gaussian function.

of each profile increased as the ground area decreased, with the result that the error of the composite profile also became higher for ground areas of less than 16 m^2. A possible reason for this error increase is that each lidar's measurement error in relation to the range accuracy became non-negligible as the ground area decreased below 16 m^2. This error increase was larger for the airborne lidar than for the portable ground-based lidar, because the range accuracy of the former is 15 cm, whereas that of the latter is 8 mm. Other possible reasons for this error increase with decreasing ground area are the heterogeneity of the canopy and the differences in the positions of the cell boundaries between the direct and lidar measurements [37]. The heterogeneity of the canopy gradually affected the error below 16 m^2. Moreover, for the stratified clipping, the cell boundaries were measured with a tape measure. As a result, slight differences in the positions of the boundaries could exist between the lidar measurements and the direct measurements, which would cause the error to become larger as the ground area became smaller. This source of error would affect measurements by both lidars. Although not caused by the lidar measurement itself, this error increases the difficulty of accurate validation of lidar-derived results. To reduce these sources of error, LAD estimation by this technique (combining the data of two types of lidar) should be used for ground areas of sufficient extent, which, in this study, corresponded to 16 m^2 or more. Because of these considerations, subsequent analyses should be done for ground areas of 16 m^2 or more.

It is obvious that a more accurate LAD estimation obtained in each lidar offers a more accurate estimation after the combination of both lidars. The LAD estimation accuracy of each lidar increases when its measurement settings such as the laser beam settings and the lidar positions are appropriately determined according to the canopy structure. The index Ω was proposed to be such a criterion for determining appropriate measurement settings. The Ω index is an indicator of the proportion of the area of a horizontal plane within the canopy covered by laser beams. This index depends on the laser beam settings (A_{beam}, N) and the canopy structural attributes $(K, \mathrm{LAI}_{\mathrm{cum}})$.

Thus, the appropriate settings can be determined according to the canopy structural attributes. When the value of Ω exceeds 1.0, the laser beams can illuminate the entire horizontal plane, but when it is less than 1.0, then some parts of the horizontal plane cannot be illuminated by the laser beams. In the former case, the LAD error decreases because the number of laser beams incident into the canopy is sufficient, but in the latter case, the error increases due to the lack of information about the canopy caused by an insufficient number of laser beams incident into the canopy. This explains the results shown in Fig. 4, in which the LAD error began to drastically increase at values of Ω near 1.0. Thus, for better LAD estimation, the value of Ω should exceed 1.0. In practice, the value of Ω should be more than 2.0 to be certain of obtaining accurate results. Therefore, in practical lidar measurements, the measurement settings such as the laser beam settings and the lidar positions should be chosen such that Ω becomes as large as possible exceeding 2.0. In addition, it is notable that a similar tendency was observed in the relationship between Ω and the LAD error for both airborne and ground-based lidars in spite of their different setting values for A_{beam} and N, as shown in Fig. 4. This means that Ω can be used to assess the LAD error of lidar measurements made by using different settings and also suggests that Ω—that is, the proportion of the area covered by laser beams in a horizontal plane—is an essential and practical factor that relates to estimation accuracy in lidar-based LAD measurements. This result indicates that Ω can be used to obtain better combinations of LAD estimates derived from different types of lidars. By comparing the values of Ω between the different types of lidars at each height, it can be determined which lidar's LAD estimate is more accurate and, thus, which LAD value should be selected.

A Gaussian function could interpolate well the underestimated part of the LAD profiles obtained by combining the results from the two types of lidar. With regard to the number of points picked up for the interpolation, the two points corresponding to the peaks of the two lidar profiles were insufficient for fitting the Gaussian function; thus, four or more points, including the two peaks, were picked up. However, the MAEs were larger when eight points were picked up, compared to the case with four or six points. In the case of eight points, the substructure of the lower layer apparently affects the form of the fitting function, resulting in an increased error. Thus, the points should be selected such that the substructure is not included, as with four and six picked-up points. The interpolation by a Gaussian function is effective when the LAD profile is monomodal, as in the present study and a previous study [49]. Monomodal profiles are typical of sites dominated by a single species [34], [49], [50]. However, at sites where several species grow, the canopy can have an LAD profile with a multimodal structure [34], [41]. For multimodal structures, interpolation can be performed by applying the fitting function to each peak separately, as suggested by a previous study [34]. The applicability of this method needs to be explored by additional works.

In future works, the applicability of the index Ω should be assessed through a wider range of scenarios. For instance, the horizontal extent of the canopy must be considered in the estimation of the LAD for a large area, and we could consider adding measurement positions for the ground-based lidar to reduce the occlusion effect. By determining the positions such that the index Ω becomes as large as possible, better estimation of LAD would be obtained. The above interpolation method would also perform well when the sufficient value of Ω cannot be obtained. In terms of laser beam penetration into the internal canopy, the size of A_{beam} in an airborne lidar should be more considered. In particular, an airborne lidar with a much smaller A_{beam} may increase the laser beam penetration through the canopy. The lidar settings (e.g., flight speed and laser scanning frequency) could properly be adjusted according to the index Ω by doing a series of tests for different A_{beam} values. It would also be significant for the applicability of the index to be tested with a lidar system based on a different measurement principle, such as a waveform-recording ground-based lidar [47]. Moreover, it would be interesting to examine whether the index is applicable to increase the accuracy of the other structural attributes of the canopy measured by lidar systems.

V. Conclusion

Vertical LAD profiles of a woody canopy have been estimated by combining airborne and portable ground-based lidar data and using the VCP method. The two data sets complemented each other, eliminating the blind regions of the two lidars and improving the accuracy of the LAD profiles. MAEs have been calculated to evaluate the method for different ground areas, and it has been shown that a ground area of sufficient extent—16 m^2 or more in the present study—yielded better results. The laser beam coverage index Ω, which incorporates the lidar laser beam settings and a laser beam attenuation factor, has been proposed. This index can predict the LAD estimation error of LAD measurements obtained by different types of lidar and with different laser beam setting values. In practical lidar-based LAD measurements, this index could be used as a criterion for determining appropriate lidar measurement settings or for obtaining a better combination of LAD profiles from different types of lidar. The underestimated part of the composite LAD profile resulting from the combination of data from the two lidars has been improved by applying Gaussian interpolation. The methods demonstrated here would be suitable for other broadleaved canopies. Coniferous canopies have different structures such as the permanent presence of foliage material for evergreen species, and the applicability of the proposed method should be examined in more detail for this type of canopy. Moreover, the effectiveness of the index Ω could be tested in additional scenarios to enhance its general applicability.

References

[1] J. L. Monteith, *Principles of Environmental Physics*. London, U.K.: Edward Arnold, 1973.

[2] H. G. Jones, *Plants and Microclimate,* 2nd ed. Cambridge, U.K.: Cambridge Univ. Press, 1992.

[3] W. Larcher, *Physiological Plant Ecology,* 4th ed. Heidelberg, Germany: Springer-Verlag, 2001.

[4] R. D. Graetz, "Remote sensing of terrestrial ecosystem structure: An ecologist's pragmatic view," in *Remote Sensing of Biosphere Functioning*, R. J. Hobbs and H. A. Mooney, Eds. New York: Springer-Verlag, 1990, pp. 5–30.

[5] M. A. Lefsky, W. B. Cohen, G. G. Parker, and D. J. Harding, "Lidar remote sensing for ecosystem studies," *Bioscience*, vol. 52, no. 1, pp. 19–30, Jan. 2002.

[6] U. Schurr, A. Walter, and U. Rascher, "Functional dynamics of plant growth and photosynthesis—From steady-state to dynamics–from homogeneity to heterogeneity," *Plant Cell Environ.*, vol. 29, no. 3, pp. 340–352, Mar. 2006.

[7] K. Omasa, F. Hosoi, and A. Konishi, "3D lidar imaging for detecting and understanding plant responses and canopy structure," *J. Exp. Bot.*, vol. 58, no. 4, pp. 881–898, Mar. 2007.

[8] M. Weiss, F. Baret, G. J. Smith, I. Jonckheere, and P. Coppin, "Review of methods for in situ leaf area index (LAI) determination Part II. Estimation of LAI, errors and sampling," *Agric. For. Meteorol.*, vol. 121, no. 1/2, pp. 37–53, Jan. 2004.

[9] M. Monsi and T. Saeki, "Über den Lichtfaktor in den Pflanzengesellschaften und seine Bedeutung für die Stoffproduktion," *Jpn. J. Bot.*, vol. 14, pp. 22–52, 1953.

[10] J. L. Drouet, B. Moulia, and R. Bonhomme, "Do changes in the azimuthal distribution of maize leaves over time affect canopy light absorption?" *Agronomie*, vol. 19, no. 3/4, pp. 281–294, Mar.–May 1999.

[11] H. Sinoquet, B. Moulia, and R. Bonhomme, "Estimating the three-dimensional geometry of a maize crop as an input of radiation models: Comparison between three-dimensional digitizing and plant profiles," *Agric. For. Meteorol.*, vol. 55, no. 3/4, pp. 233–249, Jun. 1991.

[12] H. Sinoquet, J. Stephan, G. Sonohat, P. E. Lauri, and P. Monney, "Simple equations to estimate light interception by isolated trees from canopy structure features: Assessment with three-dimensional digitized apple trees," *New Phytol.*, vol. 175, no. 1, pp. 94–106, Jul. 2007.

[13] J. M. Norman and G. S. Campbell, "Canopy structure," in *Plant Physiological Ecology: Field Methods and Instrumentation*, R. W. Pearcy, J. Ehleringer, H. A. Mooney, and P. W. Rundel, Eds. London, U.K.: Chapman & Hall, 1989, pp. 301–326.

[14] J. M. Welles and J. M. Norman, "Instrument for indirect measurement of canopy architecture," *Agron. J.*, vol. 83, no. 5, pp. 818–825, Sep./Oct. 1991.

[15] J. W. Chason, D. D. Baldocchi, and M. A. Huston, "A comparison of direct and indirect methods for estimating forest canopy leaf area," *Agric. For. Meteorol.*, vol. 57, no. 1/3, pp. 107–128, Dec. 1991.

[16] I. Jonckheere, S. Fleck, K. Nackaerts, B. Muys, P. Coppin, M. Weiss, and F. Baret, "Review of methods for in situ leaf area index determination. Part I. Theories, sensors and hemispherical photography," *Agric. For. Meteorol.*, vol. 121, no. 1/2, pp. 19–35, Jan. 2004.

[17] D. J. Harding, M. A. Lefsky, G. G. Parker, and J. B. Blair, "Laser altimeter canopy height profiles Methods and validation for closed-canopy, broadleaf forests," *Remote Sens. Environ.*, vol. 76, no. 3, pp. 283–297, Jun. 2001.

[18] T. Brandtberg, T. A. Warner, R. E. Landenberger, and J. B. McGraw, "Detection and analysis of individual leaf-off tree crowns in small footprint, high sampling density lidar data from the eastern deciduous forest in North America," *Remote Sens. Environ.*, vol. 85, no. 3, pp. 290–303, May 2003.

[19] J. Holmgren and Å. Persson, "Identifying species of individual trees using airborne laser scanner," *Remote Sens. Environ.*, vol. 90, no. 4, pp. 415–423, Apr. 2004.

[20] J. Hyyppä, O. Kelle, M. Lehikoinen, and M. Inkinen, "A segmentation-based method to retrieve stem volume estimates from 3-D tree height models produced by laser scanners," *IEEE Trans. Geosci. Remote Sens.*, vol. 39, no. 5, pp. 969–975, May 2001.

[21] E. Næsset, T. Gobakken, J. Holmgren, H. Hyyppä, J. Hyyppä, M. Maltamo, M. Nilsson, H. Olsson, Å. Persson, and U. Söderman, "Laser scanning of forest resources: The Nordic experience," *Scand. J. For. Res.*, vol. 19, no. 6, pp. 482–499, Dec. 2004.

[22] K. Omasa, Y. Akiyama, Y. Ishigami, and K. Yoshimi, "3-D remote sensing of woody canopy heights using a scanning helicopter-borne lidar system with high spatial resolution," *J. Remote Sens. Soc. Jpn.*, vol. 20, no. 4, pp. 394–406, 2000.

[23] M. Dalponte, L. Bruzzone, and D. Gianelle, "Fusion of hyperspectral and LIDAR remote sensing data for classification of complex forest areas," *IEEE Trans. Geosci. Remote Sens.*, vol. 46, no. 5, pp. 1416–1427, May 2008.

[24] R. Hecht, G. Meinel, and M. F. Buchroithner, "Estimation of urban green volume based on single-pulse LiDAR data," *IEEE Trans. Geosci. Remote Sens.*, vol. 46, no. 11, pp. 3832–3840, Nov. 2008.

[25] K. Omasa, G. Y. Qiu, K. Watanuki, K. Yoshimi, and Y. Akiyama, "Accurate estimation of forest carbon stocks by 3-D remote sensing of individual trees," *Environ. Sci. Technol.*, vol. 37, no. 6, pp. 1198–1201, Mar. 2003.

[26] K. Omasa, F. Hosoi, T. M. Uenishi, Y. Shimizu, and Y. Akiyama, "Three-dimensional modelling of an urban park and trees by combined airborne and portable on-ground scanning LIDAR remote sensing," *Environ. Model. Assess.*, vol. 13, no. 4, pp. 473–481, Nov. 2008.

[27] D. Riaño, E. Meier, B. Allgöwer, E. Chuvieco, and S. L. Ustin, "Modeling airborne laser scanning data for the spatial generation of critical forest parameters in fire behavior modeling," *Remote Sens. Environ.*, vol. 86, no. 2, pp. 177–186, Jul. 2003.

[28] J. Hyyppä and M. Inkinen, "Detecting and estimating attributes for single trees using laser scanner," *Photogramm. J. Finl.*, vol. 16, pp. 27–42, 1999.

[29] X. W. Yu, J. Hyyppä, H. Kaartinen, and M. Maltamo, "Automatic detection of harvested trees and determination of forest growth using airborne laser scanning," *Remote Sens. Environ.*, vol. 90, no. 4, pp. 451–462, Apr. 2004.

[30] S. Magnussen and P. Boudewyn, "Derivations of stand heights from airborne laser scanner data with canopy-based quantile estimators," *Can. J. For. Res.*, vol. 28, no. 7, pp. 1016–1031, Jul. 1998.

[31] F. Morsdorf, B. Kötz, E. Meier, K. I. Itten, and B. Allgöwer, "Estimation of LAI and fractional cover from small footprint airborne laser scanning data based on gap fraction," *Remote Sens. Environ.*, vol. 104, no. 1, pp. 50–61, Sep. 2006.

[32] C. J. Houldcroft, C. L. Campbell, I. J. Davenport, R. J. Gurney, and N. Holden, "Measurement of canopy geometry characteristics using LiDAR laser altimetry: A feasibility study," *IEEE Trans. Geosci. Remote Sens.*, vol. 43, no. 10, pp. 2270–2282, Oct. 2005.

[33] J. L. Lovell, D. L. B. Jupp, D. S. Culvenor, and N. C. Coops, "Using airborne and ground-based ranging lidar to measure canopy structure in Australian forests," *Can. J. Remote Sens.*, vol. 29, no. 5, pp. 607–622, Oct. 2003.

[34] N. C. Coops, T. Hilker, M. A. Wulder, B. St-Onge, G. Newnham, A. Siggins, and J. A. Trofymow, "Estimating canopy structure of Douglas-fir forest stands from discrete-return LiDAR," *Trees—Struct. Funct.*, vol. 21, no. 3, pp. 295–310, May 2007.

[35] K. Omasa, Y. Urano, H. Oguma, and Y. Fujinuma, "Mapping of tree position of *Larix leptolepis* woods and estimation of diameter at breast height (DBH) and biomass of the trees using range data measured by a portable scanning lidar," *J. Remote Sens. Soc. Jpn.*, vol. 22, no. 5, pp. 550–557, 2002.

[36] F. Hosoi, K. Yoshimi, Y. Shimizu, and K. Omasa, "3-D measurement of trees using a portable scanning lidar," *Phyton—Ann. Rei Bot. A*, vol. 45, no. 4, pp. 497–500, 2005.

[37] F. Hosoi and K. Omasa, "Voxel-based 3-D modeling of individual trees for estimating leaf area density using high-resolution portable scanning lidar," *IEEE Trans. Geosci. Remote Sens.*, vol. 44, no. 12, pp. 3610–3618, Dec. 2006.

[38] F. Hosoi and K. Omasa, "Factors contributing to accuracy in the estimation of the woody canopy leaf-area-density profile using 3D portable lidar imaging," *J. Exp. Bot.*, vol. 58, no. 12, pp. 3464–3473, Oct. 2007.

[39] F. Hosoi and K. Omasa, "Estimating vertical plant area density profile and growth parameters of a wheat canopy at different growth stages using three-dimensional portable lidar imaging," *ISRPS J. Photogramm.*, vol. 64, no. 12, pp. 151–158, Mar. 2009.

[40] P. J. Radtke and P. V. Bolstad, "Laser point-quadrat sampling for estimating foliage-height profiles in broad-leaved forests," *Can. J. Forest Res.*, vol. 31, no. 3, pp. 410–418, Mar. 2001.

[41] G. G. Parker, D. J. Harding, and M. L. Berger, "A portable LIDAR system for rapid determination of forest canopy structure," *J. Appl. Ecol.*, vol. 41, no. 4, pp. 755–767, Aug. 2004.

[42] K. Yoshimi, F. Hosoi, Y. Shimizu, H. Yamada, and K. Omasa, "3-D measurement of terrain and woody canopy height using portable scanning lidar," *Eco-Engineering*, vol. 16, no. 3, pp. 203–207, 2004.

[43] T. Tanaka, H. Park, and S. Hattori, "Measurement of forest canopy structure by a laser plane range-finding method—Improvement of radiative resolution and examples of its application," *Agric. For. Meteorol.*, vol. 125, no. 1/2, pp. 129–142, Sep. 2004.

[44] J. G. Henning and P. J. Radtke, "Ground-based laser imaging for assessing three-dimensional forest canopy structure," *Photogramm. Eng. Remote Sens.*, vol. 72, no. 12, pp. 1349–1358, Dec. 2006.

[45] T. Takeda, H. Oguma, Y. Yone, Y. Yamagata, and Y. Fujinuma, "Comparison of leaf area density measured by laser range finder and stratified clipping method," *Phyton—Ann. Rei Bot. A*, vol. 45, no. 4, pp. 505–510, 2005.

[46] T. Takeda, H. Oguma, T. Sano, Y. Yone, Y. Yamagata, and Y. Fujinuma, "Estimating the plant area density of a Japanese larch (*Larix kaempferi* Sarg.) plantation using a ground-based laser scanner," *Agric. For. Meteorol.*, vol. 148, no. 3, pp. 428–438, Mar. 2008.

[47] A. H. Strahler, D. L. B. Jupp, C. E. Woodcock, C. B. Schaaf, T. Yao, F. Zhao, X. Yang, J. Lovell, D. Culvenor, G. Newnham, W. Ni-Miester, and W. Boykin-Morris, "Retrieval of forest structural parameters using a ground-based lidar instrument (Echidna)," *Can. J. Remote Sens.*, vol. 34, pp. 426–440, 2008, Suppl.2.
[48] P. J. Besl and N. D. McKay, "A method for registration of 3-D shapes," *IEEE Trans. Pattern Anal. Mach. Intell.*, vol. 14, no. 2, pp. 239–256, Feb. 1992.
[49] J. Čermák, R. Tognetti, N. Nadezhdina, and A. Raschi, "Stand structure and foliage distribution in *Quercus pubescens* and *Quercus cerris* forests in Tuscany (central Italy)," *For. Ecol. Manag.*, vol. 255, no. 5/6, pp. 1810–1819, Apr. 2008.
[50] S. Saito, T. Sato, Y. Kominami, D. Nagamatsu, S. Kuramoto, T. Sakai, R. Tabuchi, and A. Sakai, "Modeling the vertical foliage distribution of an individual *Castanopsis cuspidata* (Thunb.) Schottky, a dominant broad-leaved tree in Japanese warm-temperate forest," *Trees—Struct. Funct.*, vol. 18, no. 4, pp. 486–491, Jul. 2004.

Fumiki Hosoi received the M.E. and Ph.D. degrees from the University of Tokyo, Tokyo, Japan, in 1995 and 2008, respectively.

In 1995, he joined the Opto-Technology Laboratory, Furukawa Electric Company, Ltd., Ichihara, Chiba, Japan. He is currently with the Graduate School of Agricultural and Life Sciences, University of Tokyo.

Yohei Nakai received the B.E. degree in 2008 from the University of Tokyo, Tokyo, Japan, where he is currently working toward the M.E. degree in the Department of Agricultural and Life Sciences.

Kenji Omasa received the M.E. degree from Ehime University, Ehime, Japan, in 1975 and the Ph.D. degree in engineering from the University of Tokyo, Tokyo, Japan.

He is currently a Professor with the Department of Agricultural and Life Sciences, University of Tokyo. His research interests include imaging of cell level to plants, remote sensing, modeling of ecosystems, analysis of global change effects on ecosystems, and information engineering for biological and environmental systems.